Neoplasia • Vol. 9, No. 10, October 2007, pp. 830–839 **830**

www.neoplasia.com

Prazosin Displays Anticancer Activity against Human Prostate Cancers: Targeting DNA and Cell Cycle

Ssu-Chia Lin[*,1], *Shih-Chieh Chueh*[†,1], *Che-Jen Hsiao*[‡], *Tsia-Kun Li*[§], *Tzu-Hsuan Chen**, *Cho-Hwa Liao**, *Ping-Chiang Lyu*[‡] *and Jih-Hwa Guh**

*School of Pharmacy, National Taiwan University, Taipei, Taiwan; [†]Department of Urology, National Taiwan University Hospital, Taipei, Taiwan; [‡]Department of Life Sciences and Institute of Bioinformatics and Structural Biology, National Tsing Hua University, Hsinchu, Taiwan; [§]Department of Microbiology, College of Medicine, National Taiwan University, Taipei, Taiwan

Abstract

Quinazoline-based α_1-adrenoceptor antagonists, in particular doxazosin and terazosin, are suggested to display antineoplastic activity against prostate cancers. However, there are few studies elucidating the effect of prazosin. In this study, prazosin displayed antiproliferative activity superior to that of other α_1-blockers, including doxazosin, terazosin, tamsulosin, and phentolamine. Prazosin induced G_2 checkpoint arrest and subsequent apoptosis in prostate cancer PC-3, DU-145, and LNCaP cells. In p53-null PC-3 cells, prazosin induced an increase in DNA strand breaks and ATM/ATR checkpoint pathways, leading to the activation of downstream signaling cascades, including Cdc25c phosphorylation at Ser^{216}, nuclear export of Cdc25c, and cyclin-dependent kinase (Cdk) 1 phosphorylation at Tyr^{15}. The data, together with sustained elevated cyclin A levels (other than cyclin B1 levels), suggested that Cdk1 activity was inactivated by prazosin. Moreover, prazosin triggered mitochondria-mediated and caspase-executed apoptotic pathways in PC-3 cells. The oral administration of prazosin significantly reduced tumor mass in PC-3–derived cancer xenografts in nude mice. In summary, we suggest that prazosin is a potential antitumor agent that induces cell apoptosis through the induction of DNA damage stress, leading to Cdk1 inactivation and G_2 checkpoint arrest. Subsequently, mitochondria-mediated caspase cascades are triggered to induce apoptosis in PC-3 cells.

Neoplasia (2007) **9,** 830–839

Keywords: Prazosin, DNA damage, cell cycle, Cdc25c, mitochondria-involved apoptosis.

Introduction

A number of discoveries have identified the molecular mechanism of apoptosis and have clarified its contribution to therapeutic outcome, in particular cancer chemotherapeutics. In the prostate, androgen deprivation substantially causes apoptosis in androgen-dependent prostate cancer cells, but not in androgen-independent tumor epithelial cells [1]. However, these nonsusceptible tumor cells undergo apoptosis with numerous chemotherapeutic agents and irradiation [2,3]. Recently, many apoptotic strategies based on different molecular mechanisms have been proposed to deal with androgen-independent prostate cancer cells. The death receptor pathway is one of the targets in apoptotic strategies. Several agents have been identified as triggering apoptosis in androgen-independent prostate cancer cells through this extrinsic apoptosis pathway, for example, valproic acid through overexpression of Fas and Fas ligand [4], coral prostanoids through Fas clustering [5], and flavonoids through induction of death receptor 5 expression [6]. Recently, tubulin has been one of the most widely studied targets. A variety of natural components and synthetic compounds have been reported to bind to tubulin, causing cell-cycle arrest and apoptosis in many types of tumor cells, including androgen-independent prostate cancer cells [7,8]. Moreover, mitochondria-involved apoptotic signaling always mutually interacts with the above pathways and explains most of the apoptotic mechanisms of chemotherapeutic agents [9–11].

α_1-Adrenoceptor antagonists are used as first-line medical treatment for patients with benign prostatic hyperplasia–related lower urinary tract symptoms. Recently, the effect of α_1-adrenoceptor antagonists on the apoptosis of both androgen-dependent and androgen-independent prostate cancer cells has been investigated. Interestingly, several lines of evidence suggest that apoptotic effect is independent of the blockade of α_1-adrenoceptors. One of the evidences suggests that apoptotic effect is specific for quinazoline-based antagonists (e.g., doxazosin and terazosin) other than sulfonamide derivatives (e.g., tamsulosin) [12,13]. Doxazosin is the most widely investigated α_1-adrenoceptor antagonist. Several signaling pathways have been identified to explain doxazosin-induced anoikis

Abbreviations: Cdk, cyclin-dependent kinase; GADD153, growth and DNA damage protein 153; GRP78, glucose-regulated protein 78; PARP, poly(ADP-ribose)polymerase; PI, propidium iodide; SRB, sulforhodamine B

Address all correspondence to: Jih-Hwa Guh, School of Pharmacy, National Taiwan University, No. 1, Section 1, Jen-Ai Road, Taipei, Taiwan. E-mail: jhguh@ntu.edu.tw

[1]Ssu-Chia Lin and Shih-Chieh Chueh contributed equally to this work.

Received 12 June 2007; Revised 11 August 2007; Accepted 14 August 2007.

DOI 10.1593/neo.07475

and cell apoptosis, namely, 1) activation of transforming growth factor-β and IκB pathways [14]; 2) inhibition of protein kinase B/Akt activation [15]; 3) induction of death receptor–mediated apoptosis [16]; 4) increase in Bax expression [17]; and 5) reduction in focal adhesion kinase [18].

There is another implication behind the discovery of doxazosin in anticancer study—"old drugs with new indication." Two advantages in this strategy are shortening of discovery time and reduction of discovery cost. Based on this strategy, we have performed large-scale anticancer screening tests in clinically used drugs with sulforhodamine B (SRB) assay, which is regularly used in the US National Cancer Institute's disease-oriented anticancer drug discovery screen. As expected, the class of α_1-adrenoceptor antagonists was able to display anticancer activity in numerous prostate cancer cell lines, including PC-3, DU-145, and LNCaP. Interestingly, prazosin (a quinazoline derivative) was more potent than doxazosin in these cancer cell lines. After the investigation of mechanism, the data showed that prazosin induced apoptotic cell death through pathways distinct from those caused by doxazosin. Furthermore, not only quinazoline-based derivatives but also imidazoline-based derivatives (i.e., phentolamine) displayed anticancer activity. In this study, anticancer mechanism and *in vivo* efficacy have been determined to demonstrate the anticancer potential of prazosin.

Materials and Methods

Materials

RPMI 1640 medium, fetal bovine serum (FBS), penicillin, streptomycin, and all other tissue culture regents were obtained from GIBCO/BRL Life Technologies (Grand Island, NY). Antibodies to GRP78 (glucose-regulated protein 78), Bcl-2, Mcl-1, Bak, Bax, poly(ADP-ribose)polymerase (PARP), cyclins A and B1, cyclin-dependent kinase (Cdk) 1, Cdk2, Cdc25c, and anti-mouse and anti-rabbit IgG were obtained from Santa Cruz Biotechnology, Inc. (Santa Cruz, CA). Antibodies to p53, phosphor-p53^{Ser15}, p21$^{Cip1/Waf1}$, p27^{Kip1}, caspase-9, caspase-8, caspase-7, phospho-Cdk1^{Tyr15}, phospho-Cdk1^{Thr161}, and Bid were obtained from Cell Signaling Technologies (Boston, MA). Antibodies to DADD153 and caspase-3 were obtained from Imgenex (San Diego, CA). Antibody to α-tubulin was obtained from Serotec Products (Beverly, MA). Antibody to *m*-calpain was obtained from BioVision (Mountain View, CA). Terminal uridine deoxynucleotidyl transferase dUTP nick end labeling (TUNEL) apoptosis detection kits were obtained from Promega (Madison, WI). Hoechst 33342, etoposide, EDTA, leupeptin, dithiothreitol, phenylmethylsulfonylfluoride, SRB, propidium iodide (PI), and all of the other chemical reagents were obtained from Sigma (St. Louis, MO).

Cell Culture

The NCI/ADR-RES cell line was obtained from the DTP Human Tumor Cell Line Screen (Developmental Therapeutics Program, National Cancer Institute). The other cancer cell lines were obtained from the American Type Culture Collection (Rockville, MD). Human cancer cells were cultured in RPMI 1640 medium with 10% FBS (vol/vol) and penicillin (100 U/ml)/streptomycin (100 μg/ml). Cultures were maintained in a humidified incubator at 37°C in 5% CO_2/95% air.

SRB Assays

Cells were seeded on 96-well plates in a medium with 5% FBS. After 24 hours, cells were fixed with 10% trichloroacetic acid to represent the cell population at the time of drug addition (T_0). After additional incubation of DMSO or drugs for 48 hours, the cells were fixed with 10% trichloroacetic acid, and SRB at 0.4% (wt/vol) in 1% acetic acid was added to stain cells. Unbound SRB was washed out by 1% acetic acid, and SRB-bound cells were solubilized with 10 mM Trizma base. Absorbance was read at a wavelength of 515 nm. Using the following absorbance measurements, such as time zero (T_0), control growth (C), and cell growth in the presence of the drug (Tx), the percentage of growth was calculated at each of the compound concentrations levels. Percent growth inhibition was calculated as: $100 - [(Tx - T_0)/(C - T_0)] \times 100$. Fifty percent growth inhibition (IC_{50}) is determined at the drug concentration that results in a 50% reduction in total protein increase in control cells during compound incubation.

In Situ *Labeling of Apoptotic Cells*

In situ detection of apoptotic cells was performed using Hoechst 33342 staining and TUNEL apoptosis detection methods. After a 36-hour treatment with or without prazosin (30 μM), the cells were washed twice with PBS, stained with Hoechst 33342 (1 μg/ml) for 15 minutes at 37°C, and fixed for 15 minutes with 4% paraformaldehyde. They were examined under a confocal laser microscopic system (Leica TCS SP2; Leica Microsystems, Mannheim, Germany). The TUNEL method identifies apoptotic cells using TdT to transfer biotin dUTP to the free 3′-OH of cleaved DNA. Biotin-labeled cleavage sites were then visualized by reaction with fluorescein-conjugated avidin. Cells were treated with or without prazosin. Then the cells were washed, fixed, and stained for apoptotic detection, in accordance with the protocol provided by Promega. Photomicrographs were obtained with a fluorescence microscope (Nikon, Tokyo, Japan).

FACScan Flow Cytometric Assay

After the treatment of cells with vehicle (0.1% DMSO) or compound for the indicated time courses, the cells were harvested by trypsinization, fixed with 70% (vol/vol) alcohol at 4°C for 30 minutes, and washed with PBS. After centrifugation, the cells were incubated in 0.1 M phosphate–citric acid buffer (0.2 M $NaHPO_4$ and 0.1 M citric acid, pH 7.8) for 30 minutes at room temperature. Then the cells were centrifuged and resuspended with 0.5 ml of PI solution containing Triton X-100 (0.1% vol/vol), RNase (100 μg/ml), and PI (80 μg/ml). DNA content was analyzed with FACScan and CellQuest software (Becton Dickinson, Mountain View, CA).

Western Blot Analysis

After the indicated exposure time of cells to DMSO or the indicated agent, cells were washed twice with ice-cold PBS

and the reaction was terminated by the addition of 100 μl of ice-cold lysis buffer (10 mM Tris–HCl pH 7.4, 150 mM NaCl, 1 mM EGTA, 1 mM phenylmethylsulfonylfluoride, 10 μg/ml aprotinin, 10 μg/ml leupeptin, and 1% Triton X-100). For Western blot analysis, the amount of proteins (40 μg) was separated by electrophoresis into a 10% or a 15% polyacrylamide gel and transferred to a nitrocellulose membrane. After an overnight incubation at 4°C in PBS/5% nonfat milk, the membrane was washed with PBS/0.1% Tween 20 for 1 hour and immunoreacted with the indicated antibody for 2 hours at room temperature. After four washings with PBS/0.1% Tween 20, the anti-mouse or anti-rabbit IgG (diluted 1:2000) was applied to the membranes for 1 hour at room temperature. The membranes were washed with PBS/0.1% Tween 20 for 1 hour, and signal detection was performed with an enhanced chemiluminescence detection kit (Amersham, Buckinghamshire, UK).

Comet Assay to Monitor the Integrity of Chromosomal DNA

Prazosin-treated or etoposide-treated cells (2×10^5; 30 minutes) were pelleted and resuspended in ice-cold PBS. The resuspended cells were mixed with 1.5% low-melting-point agarose. This mixture was loaded onto a fully frosted slide that had been precoated with 0.7% agarose, and a coverslip was then applied to the slide. The slides were submerged in prechilled lysis solution (1% Triton X-100, 2.5 M NaCl, and 10 mM EDTA, pH 10.5) for 1 hour at 4°C. After the slides had been soaked with prechilled unwinding and electrophoresis buffer (0.3 M NaOH and 1 mM EDTA) for 20 minutes, they were subjected to electrophoresis for 15 minutes at 0.5 V/cm (20 mA). After electrophoresis, the slides were stained with 1× Sybr Gold (Molecular Probes, Eugene, OR), and nuclei images were visualized and captured at 400× magnification with an Axioplan 2 fluorescence microscope (Zeiss, Tokyo, Japan) equipped with a charge-coupled device camera (Optronics, Goleta, CA). Hundreds of cells were scored to calculate the overall percentage of Comet tail–positive cells.

In Vivo *Antitumor Models*

PC-3-derived cancer xenografts in nude mice were used as an *in vivo* model. The nude mice were subcutaneously injected with PC-3 cells (10^7 cell/mouse). The tumors were measured every 2 to 3 days. When the tumors had reached a volume of 100 to 140 mm^3, the mice were divided into three groups ($n = 7$) and drug treatment was initiated. Prazosin was suspended in 0.5% carboxymethyl cellulose (CMC). Vehicle (0.5% CMC) or prazosin (3 and 10 mg/kg) was given orally every day. The length (l) and width (w) of the tumor were measured every 2 to 3 days, and tumor volume was calculated as $lw^2/2$. The protocols of the *in vivo* study were approved by the Animal Care and Use Committee at National Taiwan University.

Data Analysis

The compound was dissolved in DMSO. The final concentration of DMSO was 0.1% in cells. Data are presented as the mean ± SEM of the indicated number of separate experiments. Statistical analysis of data was performed with one-way analysis of variance followed by Bonferroni *t*-test. $P < .05$ was considered significant.

Results

Examination of the Anticancer Activities of Several α_1-Adrenoceptor Antagonists

The effect of several α_1-adrenoceptor antagonists on cell proliferation was evaluated in androgen-dependent (LNCaP) and androgen-independent (PC-3 and DU-145) prostate cancer cell lines. As demonstrated in Figure 1*A*, all of these drugs inhibited cell growth in a dose-dependent manner. The concentration of 50% inhibition on cell growth (IC_{50}) was obtained (Figure 1*B*). The data showed that prazosin was most effective, with IC_{50} values of 11.1, 16.7, and 7.5 μM in PC-3, DU-145, and LNCaP, respectively. The order of potency was as follows: prazosin > doxazosin > phentolamine > terazosin > tamsulosin. Interestingly, prazosin was two-fold more potent than doxazosin, the most widely investigated α_1-adrenoceptor antagonist [12–18]. Cell morphology was examined in PC-3 cells. The cells exhibited multinucleus features and formation of apoptotic bodies after 18 and 24 hours of treatment with prazosin, respectively (Figure 1*C*). The TUNEL reaction and Hoechst 33342 staining assays showed that prazosin induced an increase in positive staining, suggesting cell apoptosis in response to prazosin action (Figure 1*D*).

Detection of Cell-Cycle Progression and Regulators in p53-Null PC-3

Flow cytometric analysis showed that doxazosin and prazosin effectively induced an increase in sub-G_1 population (apoptosis; Figure 2*A*). Quantified data showed that prazosin, but not doxazosin, induced a concentration-dependent and time-dependent G_2/M arrest of the cell cycle and subsequent apoptosis (Figure 2, *B* and *C*). The data also demonstrated a correlation between G_2/M arrest and growth inhibition (Figure 2*B*, solid curve) in response to prazosin-mediated (other than doxazosin-mediated) effects. Accordingly, several cell-cycle regulators were examined. Cyclin A and its catalytic partner Cdk2 dominate S and G_2 phases; cyclin B1 and Cdk1 regulate cell-cycle progression from G_2 to M phase. The data demonstrated that following a 6-hour exposure to prazosin, cyclin A was upregulated and sustained at a high level. In contrast, a short-term elevation, followed by a decreased cyclin B level, was induced by prazosin (Figure 3*A*). These data were different from those by antimitotic agents. In our data (not shown), both Taxol (Sigma, Louis, MA) and vincristine (two tubulin-targeting agents) induced mitotic arrest associated with upregulation of cyclin B1 expression. Furthermore, using monoclonal antibody MPM-2 to recognize mitotic phosphoproteins, the MPM-2 expression stimulated by prazosin (30 μM), Taxol (0.1 μM), and vincristine (0.1 μM) for 24 hours was 88%, 240%, and 207%, respectively, when compared with 100% of control, revealing that prazosin did not increase MPM-2 expression. Collectively, it is

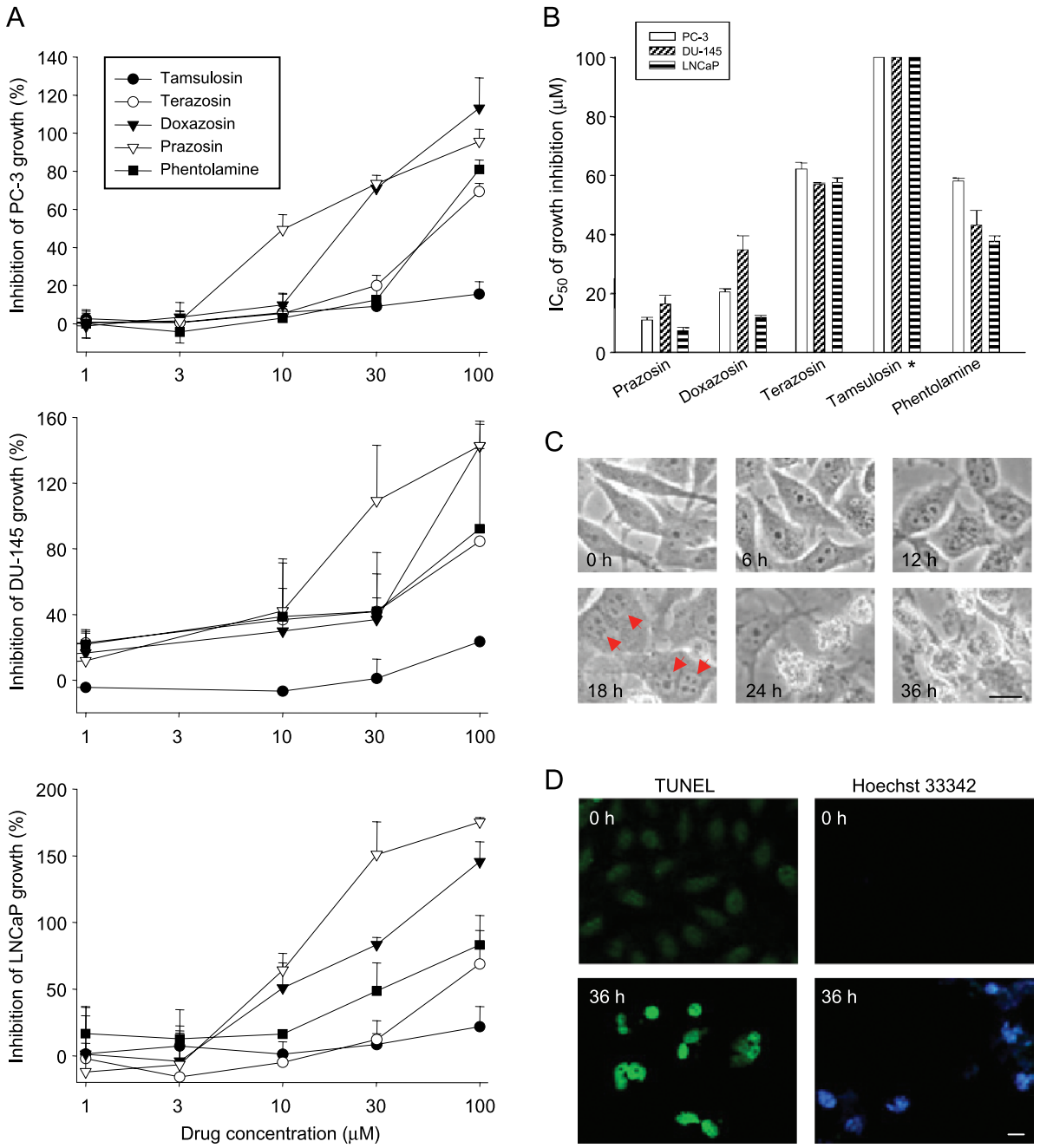

Figure 1. *Antineoplastic effect of α-adrenoceptor antagonists on several human prostate cancer cell lines. The compound, at the indicated concentration, was added to cells for 48 hours. Then the cells were fixed and stained with SRB. After a series of washings, bound SRB was subsequently solubilized and absorbance was read at a wavelength of 515 nm. Data are expressed as the mean ± SEM of four independent determinations (each in triplicate) (A). IC_{50} values were calculated as described in the Materials and Methods section (B). PC-3 cells were treated with or without prazosin (30 μM) for the indicated times. Cell morphology was detected by microscopic examination (C). PC-3 cells were treated with or without prazosin (30 μM) for 36 hours. Apoptosis was detected by TUNEL and Hoechst 33342 reaction techniques (D). Scale bar, 20 μm. *IC_{50} > 100 μM.*

suggested that prazosin induces G_2 other than the mitotic arrest of the cell cycle in PC-3.

To identify Cdk1 activity, the phosphorylation state of Cdk1 was examined because Cdk1 phosphorylation at Thr^{161} and dephosphorylation at Tyr^{15} are responsible for the activation of Cdk1 [19]. As a result, prazosin induced a time-dependent increase in Cdk1 phosphorylation at Tyr^{15}, but not at Thr^{161}, indicating inhibition of Cdk1 activity (Figure 3*B*). Several lines of evidence suggest that dephosphorylation of Cdk1 at Tyr^{15} is mainly achieved by the nuclear phosphatase Cdc25c. Chk1 and Chk2 can phosphorylate Cdc25c at Ser^{216}, which subsequently binds to 14-3-3, leading to cytoplasmic sequestration of Cdc25c [20,21]. Our data demonstrated that prazosin stimulated an increase in Cdc25c phosphorylation at Ser^{216} and a subsequent decrease in nuclear Cdc25c (Figure 3*B*). The results may explain the accumulation of phosphorylation at Tyr^{15} and the inactivation of Cdk1 in response to prazosin action.

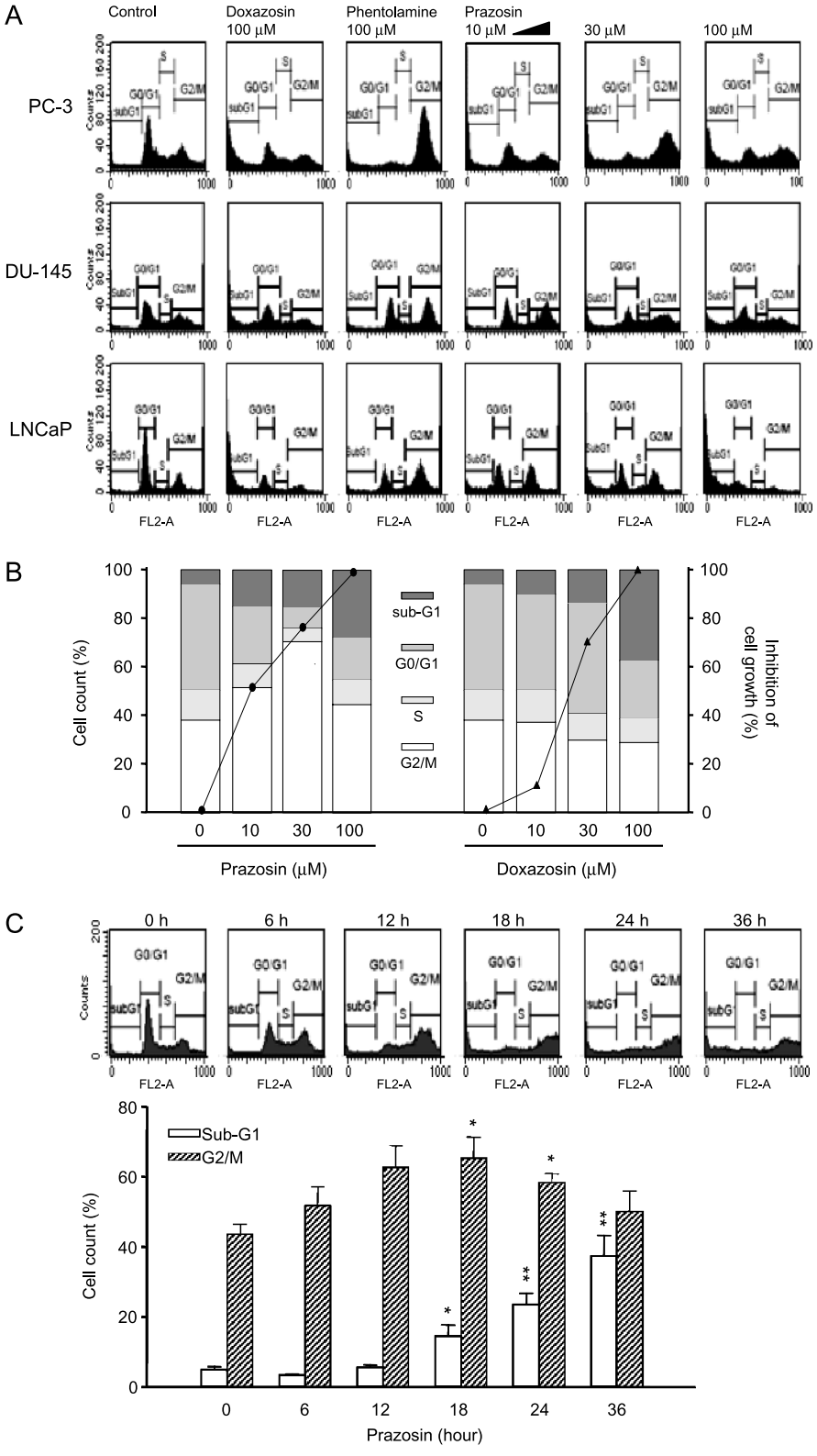

Figure 2. *Effect of α-adrenoceptor antagonists on cell-cycle progression. Cells were treated with the indicated drug at various concentrations for 48 hours. Then the cells were fixed and stained with PI to analyze DNA content by FACScan flow cytometric analysis. Data are representative of three independent experiments (A and B). The inhibition of cell growth by doxazosin and prazosin using SRB assay (solid curves) is demonstrated. The data show that growth inhibition is correlated with the population in G_2/M phase in response to prazosin action, but not with PC-3 cells in response to doxazosin action (B). Prazosin (30 μM)–mediated time-dependent change in G_2/M phase and sub-G_1 population were detected by FACScan flow cytometric analysis in PC-3 cells. Data are expressed as the mean ± SEM of three independent determinations. *P < .05 and **P < .01 compared with the respective controls (zero time) (C).*

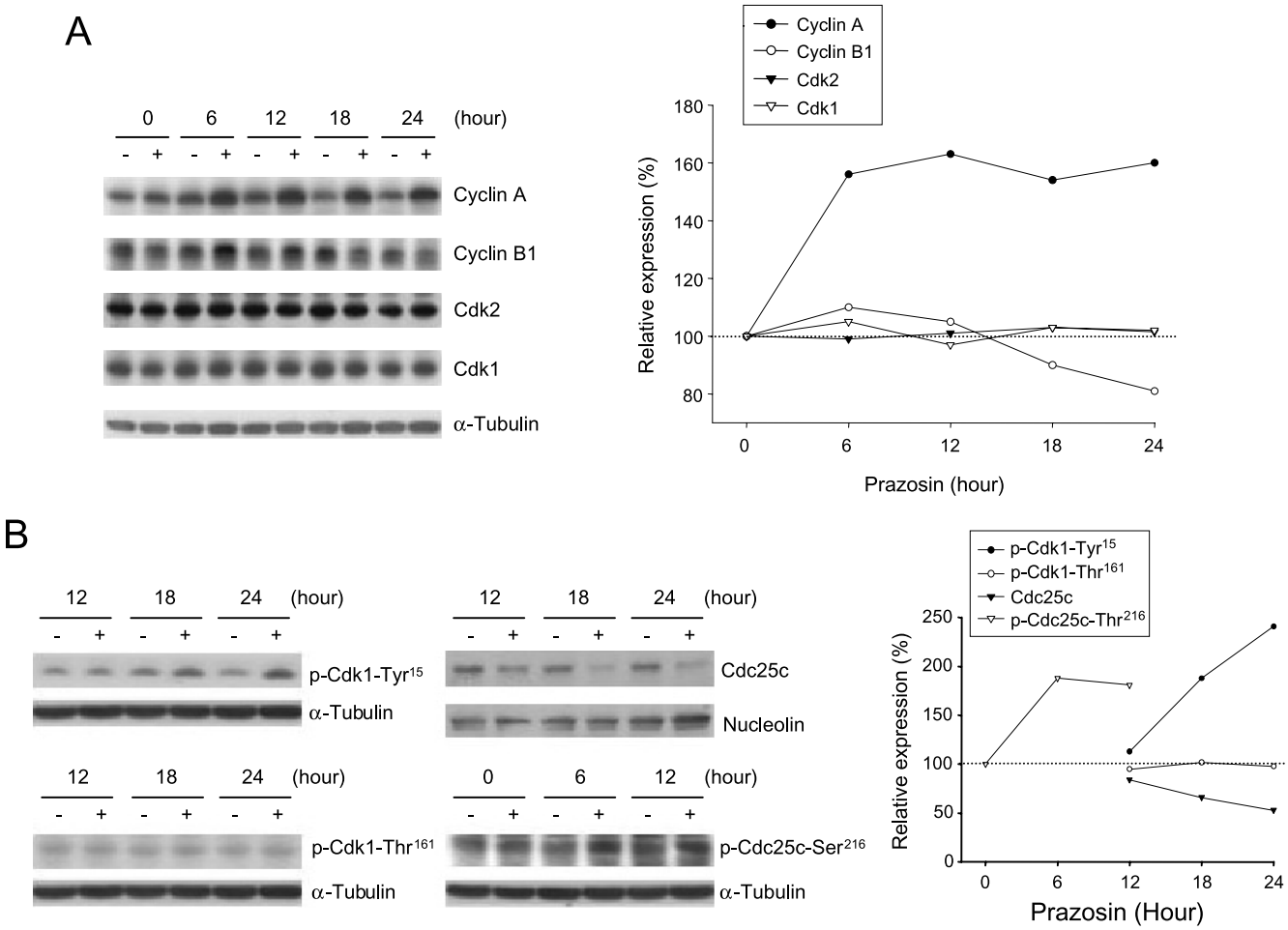

Figure 3. *Effect of prazosin on the expression of several cell-cycle regulators. (A and B) PC-3 cells were incubated in the absence or in the presence of prazosin (30 μM) for the indicated times. Then the cells were harvested and lysed for the detection of protein expression with the antibody by Western blot analysis. For Western blot analysis, the amount of proteins (40 μg) was separated by electrophoresis in a 10% or a 15% polyacrylamide gel, transferred to a nitrocellulose membrane, and immunoreacted with the indicated antibody.*

Identification of Upstream Events Contributing to Cell-Cycle Dysregulation

Caffeine, an inhibitor of ATM and ATR kinase activities, was used to examine the role of ATM and ATR kinases. As demonstrated in Figure 4*A*, caffeine was able to inhibit prazosin-mediated G_2 arrest and to restore the increased G_1 population of the cell cycle, suggesting the functional involvement of ATM and/or ATR checkpoint pathways. Furthermore, Comet assay showed that the exposure of PC-3 cells to prazosin (1 hour) induced a concentration-dependent increase in DNA strand breaks; etoposide, a topoisomerase II inhibitor, was used as a positive control (Figure 4*B*).

Determination of DNA Damage–Induced Apoptotic Signaling Cascades

An important issue of DNA damage is that it not only targets DNA but also causes stress in other cellular components, leading to amplification of apoptosis. The mitochondria and endoplasmic reticulum are two susceptible organelles [22,23]. To determine the role of endoplasmic reticulum stress, several related proteins were examined. However, prazosin neither stimulated the upregulation of GRP78 and GADD153 (growth and DNA damage protein 153) nor induced the cleavage of *m*-calpain (Figure 5*A*). Next, mitochondria-related events were examined. After a 12-hour treatment, prazosin induced the cleavage of Mcl-1 into several fragments (Figure 5*B*). It also triggered the cleavage of Bad and Bid associated with the formation of truncated fragments (Figure 5*C*). The data suggest that mitochondria are the susceptible organelles for apoptotic reaction in response to DNA damage stress.

Activation of caspases leads to the cleavage and activation/inactivation of many critical cellular substrates, including the DNA repair enzyme PARP. To determine the caspases committing prazosin-treated cells to apoptosis, the expressions of several caspases were detected by Western immunoblotting. After treatment with prazosin, the cleavage of PARP and caspases into catalytically active fragments was clearly detected in a time-dependent manner, suggesting the activation of these caspases (Figure 5*D*).

Prazosin Displays In Vivo *Antitumor Efficacy*

We subsequently carried out an *in vivo* study. The PC-3-derived cancer xenografts in nude mice were used as an

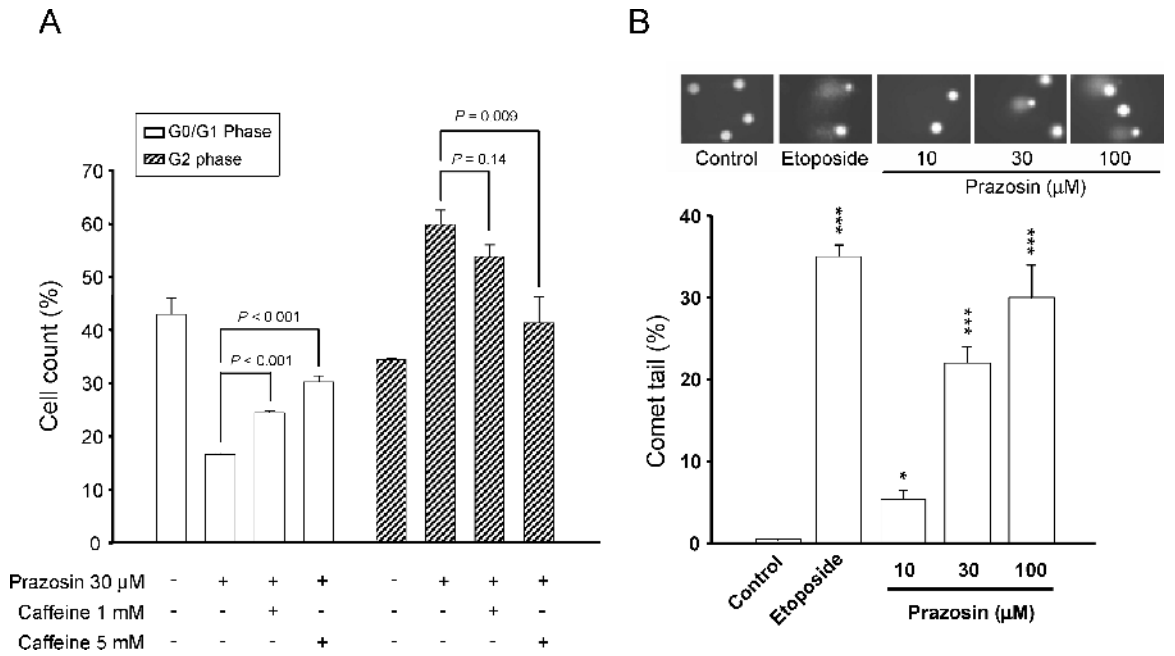

Figure 4. *Effect of prazosin on DNA damage stress in PC-3 cells. (A) Cells were treated with the indicated agent for 18 hours. Then the cells were fixed and stained with PI to analyze DNA content by FACScan flow cytometric analysis. Data are expressed as the mean ± SEM of three independent determinations. (B) Comet assay was employed to examine the integrity of chromosome DNA on treatment with prazosin (1 hour). Etoposide (50 μM) was included as a positive control. One hundred cells were scored to calculate the overall percentage of Comet tail–positive cells. Data are expressed as the mean ± SEM of three independent experiments. *P < .05 and ***P < .001 compared with controls.*

in vivo model. As demonstrated in Figure 6, oral administration of prazosin caused a significant inhibition of tumor growth without loss of body weight, indicating that prazosin under the treatment dosages had negligible toxic effect (Figure 6).

Discussion

In the past decades, numerous prospects concerning chemotherapeutic approaches to prostate cancer have emerged. Quinazoline-based α_1-adrenoceptor antagonists are suggested to display antitumor activity against prostate tumors. The apoptotic and antiangiogenic effects of doxazosin and terazosin have been widely explored [12–18]. However, prazosin, which is also a quinazoline-based α_1-blocker, does not get equal attention in anticancer approach. One of the reasons is that the plasma half-life of prazosin is shorter (about 2–4 hours) than those of terazosin (12 hours) and doxazosin (22 hours). However, the pharmacokinetic problem can be resolved by improvement of the dosage form or by multiple administrations to achieve the therapeutic plasma concentration at which prazosin shows benefits in cancer chemotherapy. In this study, prazosin showed superior inhibitory effect on proliferation in human androgen-dependent and androgen-independent prostate cancer cells.

Checkpoints are the pathways that halt the progression of cell cycle in response to cellular stress. The targets on checkpoint pathways are potential anticancer strategies because abrogation of checkpoint function drives tumor cells toward apoptosis and enhances the efficacy of oncotherapy [2,8,24]. The regulation of cell-cycle progression by prazosin is distinct from that by doxazosin. Prazosin induced G_2 checkpoint arrest before apoptosis, whereas doxazosin did not cause any checkpoint arrest of the cell cycle. Several cellular stresses may trigger checkpoint pathways, leading to cell-cycle arrest at G_2 phase. DNA damage is one of the feasible stimuli [20,21,25]. Comet assay provided evidence that prazosin induced DNA damage stress, triggering the activation of ATM/ATR checkpoint pathways. One important issue is to identify signaling cascades during DNA damage and G_2 checkpoint arrest. The cyclin B/Cdk1 complex activity is a candidate factor because it regulates cell-cycle progression from G_2 to M phase [19–21,25]. It has been well identified that Cdk1 phosphorylation at Thr^{161} and Tyr^{15} may oppositely regulate its activity. The phosphorylation at Thr^{161} (mainly by Cdk-activating kinase) is required for Cdk1 activation, whereas the phosphorylation at Tyr^{15} (mainly by Wee-1 kinase) inhibits Cdk1 activity [19]. Recently, it has been suggested that Wee-1 plays a crucial role in keeping Cdk1 inactivation and G_2 checkpoint arrest in prostate cancer cells [26]. The present work showed that prazosin induced Cdk1 phosphorylation at Tyr^{15} and downregulated cyclin B1 expression level, supporting that Cdk1 activity is inhibited by prazosin during the G_2 arrest of the cell cycle.

The regulation of Cdc25c phosphatase on Cdk1 activity has been explored. The nuclear-active Cdc25c phosphatase can remove the inhibitory phosphorylation of Cdk1 at Tyr^{15} and can activate Cdk1 activity [19–21,27]. Chk2 and Chk1 are downstream effector kinases of ATM and ATR, respectively. In response to DNA damage, activated Chk2 and Chk1 can phosphorylate Cdc25c at Ser^{216} and trigger its association with 14-3-3 protein, leading to cytoplasmic sequestration of this phosphatase [20,21]. Prazosin induced a similar pathway, including Cdc25c phosphorylation at Ser^{216} and its subsequent nuclear export. The evidence may explain

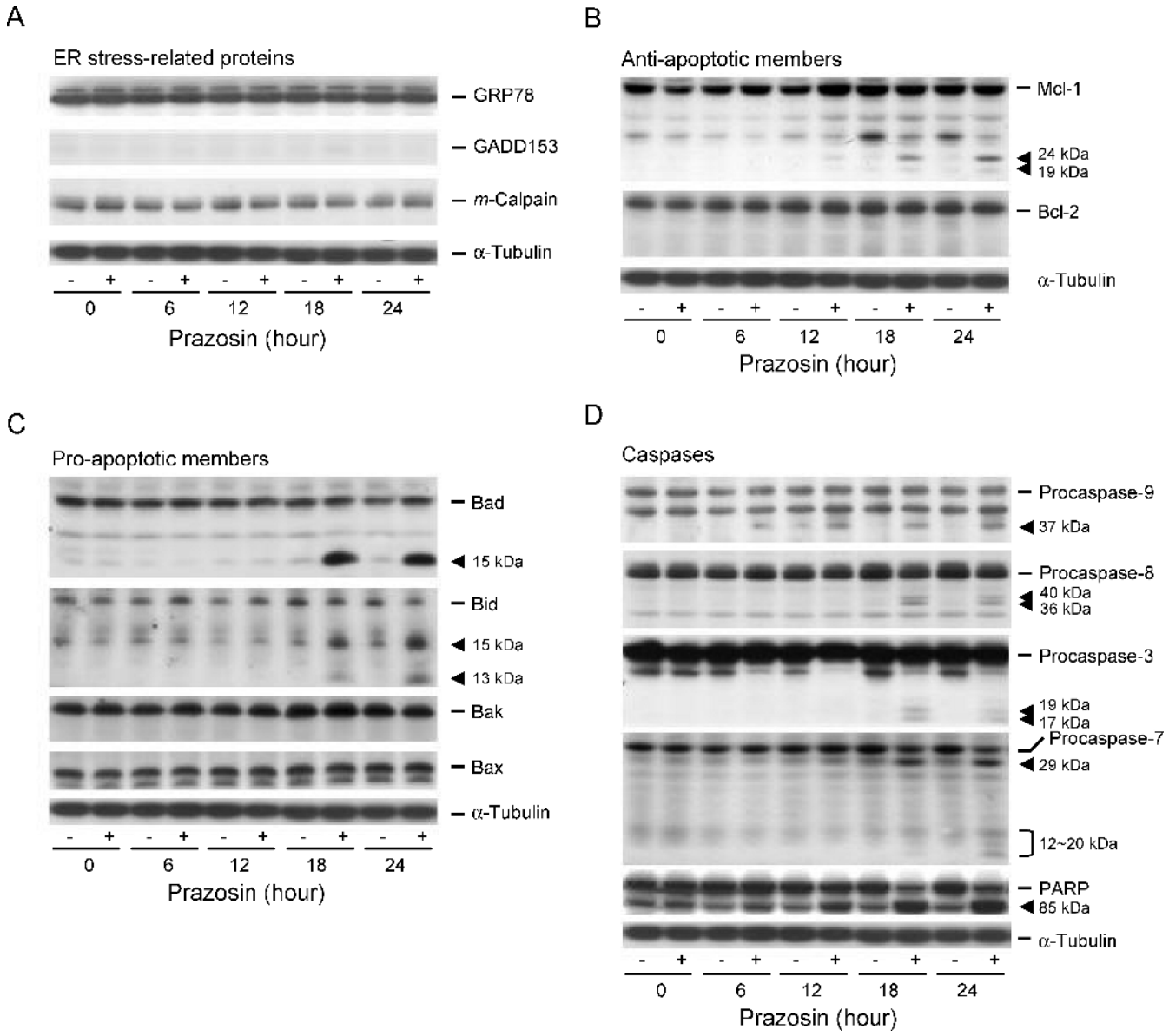

Figure 5. *Effect of prazosin on the expression of several proteins in PC-3 cells. (A–D) Cells were incubated in the absence or in the presence of prazosin (30 μM) for the indicated times. Then the cells were harvested and lysed for the detection of protein expression with the antibody by Western blot analysis. For Western blot analysis, the amount of proteins (40 μg) was separated by electrophoresis in a 10% or a 15% polyacrylamide gel, transferred to a nitrocellulose membrane, and immunoreacted with the indicated antibody.*

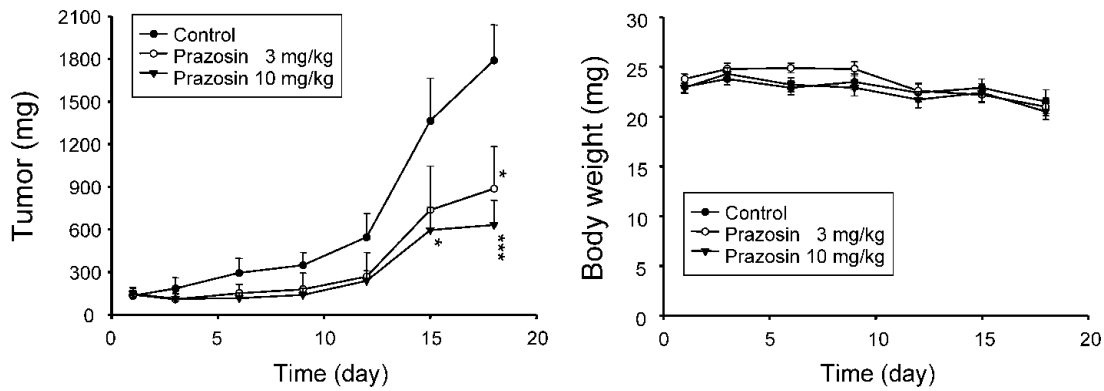

Figure 6. In vivo *antitumor study against PC-3 cells. The nude mice were subcutaneously injected with PC-3 cells (10^7 cell/mouse). The tumors were measured every 2 to 3 days. When the tumors had reached a volume of 100 to 140 mm^3, the mice were divided into three groups (n = 7), and vehicle (0.5% CMC) or prazosin (3 and 10 mg/kg) was given orally every day. Tumor volume was measured every 2 to 3 days.*

prazosin-induced increase in Cdk1 phosphorylation at Tyr^{15} and the inactivation of this kinase.

There are numerous lines of evidence suggesting that mitochondria-mediated pathways contribute to the apoptosis caused by tubulin-binding agents, topoisomerase poisons, and some other apoptotic stimuli [28–31]. Bcl-2 family protein members always play central roles in the determination of mitochondrial membrane permeability and cell survival. Mcl-1 cleavage occurring after Asp^{127} and Asp^{157} may generate four products of 24, 19, 17, and 12 kDa [32,33]. Bad and Bid, two proapoptotic Bcl-2 family members, can be cleaved into a 13-kDa and/or a 15-kDa truncated protein by caspase-3 and caspase-8, respectively [34,35]. In this study, prazosin induced the cleavage of Mcl-1, Bad, and Bid associated with the formation of truncated fragments in PC-3 cells. These effects occurred after G_2 checkpoint arrest but correlated well with the activation of caspases. The data suggest that mitochondria-mediated pathways may play a central role in prazosin-induced apoptotic mechanism in PC-3 cells.

The nude mice xenograft model was used to examine the *in vivo* antitumor potential of prazosin. The oral administration of prazosin caused a significant inhibition of tumor growth, revealing the *in vivo* efficacy of this drug. However, prazosin only induced a partial remission of tumor mass. The short plasma half-life might be one of the possibilities. Terazosin and doxazosin are two quinazoline-based related drugs with longer plasma half-lives. Nevertheless, *in vivo* α_1-adrenoceptor blocking efficacy, but not antitumor activity, is improved by these two analogues. It indicates that not only the quinazoline structure but also some other functional groups of prazosin structure are necessary for the antitumor purpose. Because the effective antitumor concentration of prazosin is high, one issue would be that the therapeutic concentration may be largely elevated. The proposal to combine therapy with radiation treatment may be performed to reduce prazosin levels. Moreover, the structure design based on prazosin may be another proposal. The discovery of new quinazoline-based chemical entities is ongoing [36].

In conclusion, the data suggest that prazosin is a potential anticancer agent that induces apoptotic signaling cascades in a sequential manner. The exposure of PC-3 cells to prazosin induces DNA damage stress and activation of ATM/ATR, leading to an increase in Cdc25c phosphorylation at Ser^{216} and the subsequent nuclear export of this phosphatase. Because of the absence of nuclear Cdc25c, a substantial increase in Cdk1 phosphorylation at Tyr^{15} results in the inactivation of Cdk1 and G_2 checkpoint arrest. Subsequently, mitochondria-mediated pathways are triggered by the cleavage of the Bcl-2 family of proteins. Finally, caspase cascades are activated to execute apoptotic cell death in response to prazosin action.

Acknowledgements

We acknowledge the support provided by the National Science Council of the Republic of China (NSC 96-2323-B-002-004 and NSC 95-2323-B-002-006).

References

[1] Kyprianou N, English HF, and Isaacs JT (1990). Programmed cell death during regression of PC-82 human prostate cancer following androgen ablation. *Cancer Res* **50**, 3748–3753.

[2] Efstathiou E, Bozas G, Kostakopoulos A, Kastritis E, Deliveliotis C, Antoniou N, Skarlos D, Papadimitriou C, Dimopoulos MA, and Bamias A (2005). Combination of docetaxel, estramustine phosphate, and zoledronic acid in androgen-independent metastatic prostate cancer: efficacy, safety, and clinical benefit assessment. *Urology* **65**, 126–130.

[3] Martel CL, Gumerlock PH, Meyers FJ, and Lara PN (2003). Current strategies in the management of hormone refractory prostate cancer. *Cancer Treat Rev* **29**, 171–187.

[4] Angelucci A, Valentini A, Millimaggi D, Gravina GL, Miano R, Dolo V, Vicentini C, Bologna M, Federici G, and Bernardini S (2006). Valproic acid induces apoptosis in prostate carcinoma cell lines by activation of multiple death pathways. *Anticancer Drugs* **17**, 1141–1150.

[5] Chiang PC, Kung FL, Huang DM, Li TK, Fan JR, Pan SL, Shen YC, and Guh JH (2006). Induction of Fas clustering and apoptosis by coral prostanoid in human hormone-resistant prostate cancer cells. *Eur J Pharmacol* **542**, 22–30.

[6] Horinaka M, Yoshida T, Shiraishi T, Nakata S, Wakada M, and Sakai T (2006). The dietary flavonoid apigenin sensitizes malignant tumor cells to tumor necrosis factor–related apoptosis-inducing ligand. *Mol Cancer Ther* **5**, 945–951.

[7] Ramaswamy B and Puhalla S (2006). Docetaxel: a tubulin-stabilizing agent approved for the management of several solid tumors. *Drugs Today (Barcelona)* **42**, 265–279.

[8] Zhou J, Liu M, Aneja R, Chandra R, and Joshi HC (2004). Enhancement of paclitaxel-induced microtubule stabilization, mitotic arrest, and apoptosis by the microtubule-targeting agent EM012. *Biochem Pharmacol* **68**, 2435–2441.

[9] Wendt J, von Haefen C, Hemmati P, Belka C, Dorken B, and Daniel PT (2005). TRAIL sensitizes for ionizing irradiation-induced apoptosis through an entirely Bax-dependent mitochondrial cell death pathway. *Oncogene* **24**, 4052–4064.

[10] Lu PH, Kung FL, Kuo SC, Chueh SC, and Guh JH (2006). Investigation of anti-tumor mechanisms of K2154: characterization of tubulin isotypes, mitotic arrest and apoptotic machinery. *Naunyn Schmiedeberg's Arch Pharmacol* **374**, 223–233.

[11] Hu H, Jiang C, Schuster T, Li GX, Daniel PT, and Lu J (2006). Inorganic selenium sensitizes prostate cancer cells to TRAIL-induced apoptosis through superoxide/p53/Bax–mediated activation of mitochondrial pathway. *Mol Cancer Ther* **5**, 1873–1882.

[12] Benning CM and Kyprianou N (2002). Quinazoline-derived α_1-adrenoceptor antagonists induce prostate cancer cell apoptosis *via* an α_1-adrenoceptor–independent action. *Cancer Res* **62**, 597–602.

[13] Tahmatzopoulos A, Rowland RG, and Kyprianou N (2004). The role of α-blockers in the management of prostate cancer. *Expert Opin Pharmacother* **5**, 1279–1285.

[14] Partin JV, Anglin IE, and Kyprianou N (2003). Quinazoline-based α_1-adrenoceptor antagonists induce prostate cancer cell apoptosis *via* TGF-β signaling and I kappa B α induction. *Br J Cancer* **88**, 1615–1621.

[15] Shaw YJ, Yang YT, Garrison JB, Kyprianou N, and Chen CS (2004). Pharmacological exploitation of the α_1-adrenoreceptor antagonist doxazosin to develop a novel class of antitumor agents that block intracellular protein kinase B/Akt activation. *J Med Chem* **47**, 4453–4462.

[16] Garrison JB and Kyprianou N (2006). Doxazosin induces apoptosis of benign and malignant prostate cells *via* a death receptor-mediated pathway. *Cancer Res* **66**, 464–472.

[17] Chiang CF, Son EL, and Wu GJ (2005). Oral treatment of the TRAMP mice with doxazosin suppresses prostate tumor growth and metastasis. *Prostate* **64**, 408–418.

[18] Walden PD, Globina Y, and Nieder A (2004). Induction of anoikis by doxazosin in prostate cancer cells is associated with activation of caspase-3 and a reduction of focal adhesion kinase. *Urol Res* **32**, 261–265.

[19] Castedo M, Perfettini JL, Roumier T, and Kroemer G (2002). Cyclin-dependent kinase-1: linking apoptosis to cell cycle and mitotic catastrophe. *Cell Death Differ* **9**, 1287–1293.

[20] Graves PR, Lovly CM, Uy GL, and Piwnica-Worms H (2001). Localization of human Cdc25C is regulated both by nuclear export and 14-3-3 protein binding. *Oncogene* **20**, 1839–1851.

[21] Karlsson-Rosenthal C and Millar JB (2006). Cdc25: mechanisms of checkpoint inhibition and recovery. *Trends Cell Biol* **16**, 285–292.

[22] Bruneel A, Labas V, Mailloux A, Sharma S, Royer N, Vinh J, Pernet P, Vaubourdolle M, and Baudin B (2005). Proteomics of human umbilical vein endothelial cells applied to etoposide-induced apoptosis. *Proteomics* **5**, 3876–3884.

[23] Szegezdi E, Logue SE, Gorman AM, and Samali A (2006). Mediators of endoplasmic reticulum stress–induced apoptosis. *EMBO Rep* **7**, 880–885.

[24] Savickiene J, Borutinskaite VV, Treigyte G, Magnusson KE, and Navakauskiene R (2006). The novel histone deacetylase inhibitor BML-210 exerts growth inhibitory, proapoptotic and differentiation stimulating effects on the human leukemia cell lines. *Eur J Pharmacol* **549**, 9–18.

[25] Jeggo PA and Lobrich M (2006). Contribution of DNA repair and cell cycle checkpoint arrest to the maintenance of genomic stability. *DNA Repair (Amsterdam)* **5**, 1192–1198.

[26] Touny LH and Banerjee PP (2006). Identification of both Myt-1 and Wee-1 as necessary mediators of the p21-independent inactivation of the cdc-2/cyclin B1 complex and growth inhibition of TRAMP cancer cells by genistein. *Prostate* **66**, 1542–1555.

[27] Nilsson I and Hoffmann I (2000). Cell cycle regulation by the Cdc25 phosphatase family. *Prog Cell Cycle Res* **4**, 107–114.

[28] Shiah HS, Lee WS, Juang SH, Hong PC, Lung CC, Chang CJ, Chou KM, and Chang JY (2007). Mitochondria-mediated and p53-associated apoptosis induced in human cancer cells by a novel selenophene derivative, D-501036. *Biochem Pharmacol* **73**, 610–619.

[29] Wang LG, Liu XM, Kreis W, and Budman DR (1999). The effect of antimicrotubule agents on signal transduction pathways of apoptosis: a review. *Cancer Chemother Pharmacol* **44**, 355–361.

[30] Sordet O, Khan QA, Kohn KW, and Pommier Y (2003). Apoptosis induced by topoisomerase inhibitors. *Curr Med Chem Anticancer Agents* **3**, 271–290.

[31] Caruso F, Villa R, Rossi M, Pettinari C, Paduano F, Pennati M, Daidone MG, and Zaffaroni N (2007). Mitochondria are primary targets in apoptosis induced by the mixed phosphine gold species chlorotriphenylphosphine-1,3-bis(diphenylphosphino) propanegold(I) in melanoma cell lines. *Biochem Pharmacol* **73**, 773–781.

[32] Michels J, Johnson PW, and Packham G (2005). Mcl-1. *Int J Biochem Cell Biol* **37**, 267–271.

[33] Herrant M, Jacquel A, Marchetti S, Belhacene N, Colosetti P, Luciano F, and Auberger P (2004). Cleavage of Mcl-1 by caspases impaired its ability to counteract Bim-induced apoptosis. *Oncogene* **23**, 7863–7873.

[34] Condorelli F, Salomoni P, Cotteret S, Cesi V, Srinivasula SM, Alnemri ES, and Calabretta B (2001). Caspase cleavage enhances the apoptosis-inducing effects of BAD. *Mol Cell Biol* **21**, 3025–3036.

[35] Ward MW, Rehm M, Duessmann H, Kacmar S, Concannon CG, and Prehn JH (2006). Real time single cell analysis of Bid cleavage and Bid translocation during caspase-dependent and neuronal caspase-independent apoptosis. *J Biol Chem* **281**, 5837–5844.

[36] Antonello A, Hrelia P, Leonardi A, Marucci G, Rosini M, Tarozzi A, Tumiatti V, and Melchiorre C (2005). Design, synthesis, and biological evaluation of prazosin-related derivatives as multipotent compounds. *J Med Chem* **48**, 28–31.